Cellular Physiology and Biochemistry

Cell Physiol Biochem 2019;52:1484-1502
DOI: 10.33594/000000103
Published online: 18 May 2019
Accepted: 14 May 2019

Original Paper

Renal Fibrosis, Immune Cell Infiltration and Changes of TRPC Channel Expression after Unilateral Ureteral Obstruction in *Trpc6*$^{-/-}$ Mice

Weiying Kong[a,b,c,d] Timo Nicolas Haschler[a,d,e] Bernd Nürnberg[b,c]
Stephanie Krämer[d,f] Maik Gollasch[a,g] Lajos Markó[a]

[a]Experimental and Clinical Research Center (ECRC), Charité Medical Faculty and Max-Delbrück Center for Molecular Medicine, Berlin, Germany, [b]Department of Pharmacology and Experimental Therapy, Institute of Experimental and Clinical Pharmacology and Toxicology, Eberhard Karls University Hospitals and Clinics, Tübingen, Germany, [c]Interfaculty Center of Pharmacogenomics and Drug Research, University of Tübingen, Tübingen, Germany, [d]Max-Rubner-Laboratory, German Institute of Human Nutrition Potsdam-Rehbrücke, Nuthetal, Germany, [e]Centre for Nephrology, UCL Medical School, Royal Free Campus, London, United Kingdom, [f]Department of Laboratory Animal Science and Animal Welfare, Justus-Liebig University Giessen, Giessen, Germany, [g]Charité Campus Virchow, Nephrology/ Intensive Care, Berlin, Germany

Key Words
Trpc channels • TRPC6 • UUO • Renal fibrosis • Inflammatory infiltration

Abstract
Background/Aims: The transient receptor potential cation channel subfamily C member 6 (TRPC6) is a Ca^{2+}-permeable nonselective cation channel and has received recent attention because of its capability to promote chronic kidney disease (CKD). The aims of this study were (i) to examine whether deletion of TRPC6 impacts on renal fibrosis and inflammatory cell infiltration in an early CKD model of unilateral ureter obstruction (UUO) in mice; and (ii) whether TRPC6-deficiency as well as UUO affect the regulation of TRPC expression in murine kidneys. ***Methods:*** Wild-type (WT), *Trpc6*-knockout (*Trpc6*$^{-/-}$) and New Zealand obese (NZO) mice underwent sham operation or unilateral ureteral obstruction (UUO). The kidneys were harvested 7 days after surgery. We examined renal fibrosis and inflammatory cell infiltration by histological and immunohistochemical staining. The mRNA expression of TRPC members and markers of fibrosis and inflammation in kidney were assessed by using real-time quantitative reverse transcription PCR. ***Results:*** Histological and immunohistochemical analyses revealed less inflammatory cell infiltration (F4/80 and CD3) in UUO kidneys of *Trpc6*$^{-/-}$ mice compared to UUO kidneys of WT mice as well as less fibrosis. Genomic deletion of TRPC6 also affected the

W. Kong and T. N. Haschler contributed equally to this work.

Lajos Markó, MD, PhD
Maik Gollasch MD, PhD
Experimental and Clinical Research Center (ECRC), Charité Medical Faculty and Max-Delbrück Center for Molecular Medicine, Lindenberger Weg 80, Berlin, 13125 (Germany)
Tel. +49-030-450-540144, +49-030-450-540177, E-Mail lajosmarko@yahoo.com, maik.gollasch@charite.de

expression of pro-fibrotic genes in UUO *Trpc6*$^{-/-}$ kidneys compared to UUO WT kidneys while the expression of pro-inflammatory genes did not differ. UUO caused marked up-regulation of *Trpc6* and down-regulation of *Trpc1* mRNA in kidneys of WT and NZO mice. *Trpc3* mRNA expression was significantly elevated in kidneys of *Trpc6*$^{-/-}$ mice underwent UUO while the levels did not change in kidneys of neither WT nor in NZO mice underwent UUO. ***Conclusion:*** TRPC6 contributes to renal fibrosis and immune cell infiltration in the UUO mouse model. Therefore, inhibition of TRPC6 emerges as a promising novel therapeutic strategy for treatment of chronic kidney failure in chronic obstructive nephropathy. However, confounding genomic and non-genomic effects of other TRPC channels should be taken into consideration to fully comprehend the renoprotective potential of targeting TRPC6 therapeutically under chronic kidney damaging conditions.

Introduction

Renal fibrosis is the inevitable consequence of an excessive accumulation of extracellular matrix that occurs in virtually every type of chronic kidney disease (CKD) irrespective of the underlying etiology [1]. Renal fibrosis is the principal process underlying the progression of CKD to end-stage renal disease. It is characterized by glomerulosclerosis and tubulointerstitial fibrosis, and by deposition of excess matrix in the interstitial space surrounding tubules and peritubular capillaries, coupled with the appearance of interstitial fibroblasts [2]. The initiation and progression of renal fibrosis appear to involve a complex, so far incompletely characterized, interaction between injured tubules, pericytes, fibroblasts, endothelial cells and inflammatory cells [2, 3]. Considerable efforts are being made to identify novel drug targets to prevent or halt renal fibrosis, the final common pathway of a wide variety of CKD.

The unilateral ureteral obstruction (UUO) model is a standard and widely used experimental model of renal interstitial fibrosis (for review see [4]). Ureteral obstruction results in marked renal hemodynamic and metabolic changes, followed by tubular injury and cell death by apoptosis or necrosis, in conjunction with an infiltration of macrophages and other inflammatory cells into the renal interstitium. Proliferation of fibroblasts and transformed myofibroblasts produce excessive extracellular matrix leading to accelerated renal fibrosis. Phenotypic transition of resident renal tubular cells, endothelial cells, and pericytes has also been implicated in this process [4].

Transient receptor potential (TRP) channels have been implicated in renal fibrosis. The classical or canonical TRP channels (TRPCs) are the subfamily most closely related to the founding member of the TRP family, the Drosophila TRP channel [5, 6]. TRPCs are Ca^{2+}-permeable nonselective cation channels encoded by *Trpc1-7*. While most TRPC subunits can form functional homomeric channels, heteromerization of TRPC channel subunits of either the same subfamily or different subfamilies has been widely observed to extend functional diversity [7-12].

TRPC6 is widely expressed in renal tissues, including glomerular podocytes, mesangial cells, endothelial cells, tubulointerstitial vascular and epithelial cells, as well as renal blood vessels [13]. TRPC6 is one of the podocyte slit-diaphragm proteins associated with proteinuria, which is mainly mediated by Ca^{2+} influx [14]. TRPC6, nephrin, podocin and CD2-associated protein directly or indirectly interact with α-actinin-4 to maintain the integrity of the glomerular filtration barrier [14, 15]. Podocyte TRPC6 channels play a role in inherited focal segmental glomerulosclerosis (FSGS) [6]. Moreover, angiotensin II (Ang II), known as an important causal driver of chronic kidney disease, can rapidly activate and upregulate the expression of TRPC6 in podocytes. As a result, the intracellular Ca^{2+} concentration increases and eventually leads to podocyte apoptosis and progressive kidney failure [16, 17].

Interestingly, up-regulation of both TRPC3 and TRPC6 expression has been reported in UUO kidneys [18]. It is suggested that up- or downregulation of other TRPCs could possibly play critical roles in kidneys. For another example, diabetic kidneys show reduced TRPC1 expression [19], which together with increased TRPC6 activity in podocytes could

contribute to glomerulopathy [20-22]. Given that the TRPCs have the ability to form homo- and heteromers, it is very likely that other TRPC family members additionally contribute to the formation of nephropathy in mouse and man.

The metabolic syndrome characterized by hypertension, hypoglycemia and lipedema is a complex disease leading to chronic kidney disease and fibrosis, as well. The New Zealand Obese (NZO) mouse represents one of the most thoroughly investigated polygenic models for the human metabolic syndrome and type 2 diabetes. It presents the main characteristics of the disease complex, including early-onset obesity, insulin resistance, dyslipidemia, and hypertension [23-25]. To the best of our knowledge, no studies have been reported on renal expression of TRPC channels in this model and their putative role in CKD progression.

We tested the hypothesis that up-regulation of renal TRPC6 is a common feature in renal fibrosis and immune cell infiltration in mice. We used the UUO model to induce renal fibrosis, immune cell infiltration and analyzed the expression of TRPC channels in the kidneys of wild-type (WT) and *Trpc6*-knockout (*Trpc6*$^{-/-}$) mice. Further we used the NZO mouse model [23-26] to evaluate UUO nephropathy as well as the regulation of TRPC channel expression in an inbred obese mouse strain carrying susceptibility genes for diabetes and hypertension.

Materials and Methods

Animals

Male *Trpc6*$^{-/-}$ mice (24.51±2.73 g body weight (b.w.), n=31, 9-12 weeks old) and age-matched WT controls (25.69±1.79 g b.w., n=32, $p>0.05$) were used. The *Trpc6*$^{-/-}$ mice have been generated on C57BL/6J:129/Sv genetic background and characterized previously [27]. Since 129Sv and C57BL/6J mice display similar renal damage in the UUO-model [28], we chose C57BL/6J mice as control *Trpc6*$^{+/+}$ (WT) mice. Age-matched male NZO mice from our own colony were used, which were obese (39.90±4.11 g b.w., n=15, $p<0.05$ vs. both WT and *Trpc6*$^{-/-}$ mice) and carry susceptibility genes (from the NZO/BomHIDife genetic background) for obesity, diabetes and hypertension [23-26]. The mice were housed in groups of three to five and single housing was applied 7 days before and after the UUO surgery to assure uniformity. The mice were reared under specific pathogen free (SPF)-conditions in individually ventilated cages (IVC) with a diurnal 12 h light and dark cycle (lights on at 06:00 h) at a temperature of 21±1°C. All animals had free access to water and food. The mice were housed and handled in unity with good animal practice as defined by the Federation of European Laboratory Animal Science Associations (FELASA) [29] and the national welfare body GV-SOLAS [30]. Animal care followed American Physiological Society guidelines [31]. All animal protocols were approved by local authorities (Landesamt für Umwelt, Gesundheit und Verbraucherschutz (LUGV) Brandenburg, Germany; Permit-Number: 2347-7-2016).

UUO model

All surgical procedures were performed under aseptic conditions. The mice were anesthetized with 2% isoflurane and placed on a heating pad to prevent hypothermia. After the depth of anaesthesia was confirmed by a loss of reflexes (toe pinch) the anterior abdominal skin was shaved, wiped off with 70% ethanol and 500 mg/kg metamizole (500 mg/ml, WDT) was injected intraperitoneally (i.p.). Eventually a midline laparotomy was conducted via an incision of the avascular linea alba and the left ureter was exposed. The ureter was then ligated twice close to the renal pelvis using a 5-0 polyglycolic acid (PGA) suture wire (Resorba®), and subsequently, 0.05 ml of a 10% enrofloxacine solution (Baytril, Bayer) was applied in the abdominal cavity. Sham operation was performed without ureteral ligation. The linea alba and skin were closed separately. The wound was sanitized with a silver aluminium spray (Henry Schein®) and 1 ml of warm (37°C) isotonic sodium chloride solution (Berlin-Chemie Menarini) was injected subcutaneously (s.c.). Subsequently, each mouse was placed in a cage in front of an infrared (IR) lamp and monitored until they recovered consciousness. For the following two days mice received metamizole (500 mg/ml, Lichtenstein) in their drinking water with a final concentration of 1.33 mg/ml. The tissue harvest occurred 7 days after the surgeries (UUO and sham). For this, mice where sacrificed with an overdose of isoflurane (1 ml/ml, CP-Pharma) and death was confirmed via a lack of reflex formation upon targeted provocation. Left kidneys were excised and decapsulated for further analysis. The kidneys were transversely divided into two

portions. Half of the kidney was immersed in a 4% phosphate-buffered paraformaldehyde (PFA) (Sigma) solution for histology, and the other half was snap-frozen in liquid nitrogen for RNA preparation.

Histology, immunohistochemistry and histological analyses

Paraffin-embedded kidneys were cut in three micrometer thick sections followed by deparaffination in sequential steps of xylene, ethanol solutions (100%, 96%, 70%) and a final rehydration step in water. For the morphological and histological analyses, Sirius red (SR) stains and Periodic acid Schiff (PAS) reactions were performed according to the manufacturer's protocols (Sigma). SR specifically stains collagen type 1 and 3 fibrils and allows a quantification of interstitial fibrosis. The PAS reaction visualizes the basement membranes of the capillary loops of the glomeruli through which the glomerular damage can be evaluated.

For the immunohistochemical (IHC) analysis and detection of proteins of interest the following procedure was conducted: Antigen retrieval was achieved by immersing the samples in boiling sodium citrate buffer (MW-buffer, pH 6.0, S2031, DAKO) in a microwave. This included two 4 min steps and a 5 min step at room temperature in between. In order to block the endogenous peroxidase activity, the tissues were incubated in 3% H_2O_2 in purified water for 10 min. Furthermore, the tissue was perforated using Tris-buffered saline with tween 20 (TBST) buffer for 15 min and potential unspecific antibody binding was prevented via a 10 min blocking step with DAKO antibody diluent (S3022, DAKO). In between each of these steps, the samples were washed with a TBST buffer for 5 min and a final washing step with phosphate-buffered saline (PBS) before the incubation with the following primary antibodies: anti-F4/80 (rat monoclonal, 1:8000, MCA497GA, Serotec), anti-CD3 (rabbit polyclonal, 1:250, ab5690, Abcam), anti-alpha smooth muscle actin (αSMA) (rabbit polyclonal, 1:500, ab5694, Abcam), anti-vimentin (rabbit monoclonal, 1:2000, ab92547, Abcam), collagen type 4, alpha 1 (Col4α1) (rabbit polyclonal, 1:2000, ab6586, Abcam), anti-proliferating cell nuclear antigen (PCNA) (rabbit polyclonal, 1:1000, ab18197, Abcam) and anti-cleaved-caspase 3 (cCasp3) (rabbit polyclonal, 1:280, 9661S, Cell Signaling). The specificity of the antibodies was ensured by negative and positive controls, as well as secondary antibody controls. All primary antibodies were diluted in DAKO antibody diluent and incubated over night at 4 °C – except for the anti-CD3 antibody whose incubation occurred at room temperature for 1 hour (h). After antibody incubation, the samples were washed three times with PBS (5 min each) and Histofine® Simple Stain™ MAX PO, which uses the 3, 3'-diaminobenzidine (DAB) chromogen, was applied according to the manufacturer's protocol (Nichirei). This allowed the visualization of the proteins of relevance. Eventually, the tissue samples were counterstained with haematoxylin (Roth) and dehydrated in a sequence of ethanol solutions followed by a final xylene dehydration step. The slides were then sealed with mounting medium (Histokitt, 1025/500, Hecht) and stored until they were imaged.

The kidneys of all animals in each group were analyzed in a blinded manner to minimize the observer bias. Images were taken with an Axio Imager.A1 (Zeiss) microscope at either 20x (all IHC stains) or 40x (PAS and SR). The cortex of each kidney sample was screened thoroughly starting at one end of the tissue and ending at the other. In order to achieve a concise quantification of the area of interest in a semiautomatic manner we used an NIH ImageJ plug-in, which has previously been generated by Gabriel Landini (University of Birmingham). This plug-in allows a colour threshold to be set and moreover, the generation of macros that can be individually applied to all stored images of each stain to guarantee consistency. The mesangial expansion and thus glomerular damage could be visualized with the PAS stain. For this, the PAS^+ area of at least 20 glomeruli in each animal was analysed. This was done by assessing the glomerular perimeter and normalizing the positively stained area to the glomerular capillary tuft area. The SR stain allowed the quantification of fibrosis in the renal cortex. At least 15 pictures of each SR-stained kidney were taken and the total positively stained area of each visual field was quantified. The F4/80, vimentin, αSMA, Col4α1 positive areas were measured in the same manner whereas $CD3^+$ as well as $PCNA^+$ cells were counted individually using the ImageJ threshold plug-in as previously mentioned.

Quantitative Real-Time (qRT)-PCR.

qRT-PCR was performed as described earlier [32]. Briefly, total RNA was isolated from snap-frozen kidney cortex after homogenization with a Precellys 24 homogenizer (Peqlab) using RNeasy RNA isolation kit (Qiagen). RNA quality and concentration were determined by a NanoDrop-1000 spectrophotometer (Thermo Fisher Scientific). Two micrograms of total renal RNA were transcribed to cDNA (Applied Biosystems). Quantitative analysis of target mRNA expression was calculated using the relative standard curve method. TaqMan and SYBR green analysis was conducted using an Applied Biosystems 7500 Sequence

Detector (Applied Biosystems). The expression levels were normalized to GAPDH (glyceraldehyde-3-phosphate dehydrogenase) and eEF1α1 (eukaryotic translation elongation factor 1 alpha 1) and mean Ct values of each groups are reported (Supplementary Fig. 1). Primer sequences are provided in Supplementary Table 1 - for all supplemental material see www.cellphysiolbiochem.com

Statistical analyzes

Statistical analyses were performed using GraphPad Prism 7.0 (GraphPad Software). All data are presented as mean ± SD and *p*-values of <0.05 were considered as statistically significant. The *p*-values in the figures are denoted as follows: ns *p>0.05*, **p*<0.05, ***p*<0.01, ****p*<0.001 and *****p*<0.0001. Data were analyzed by regular two-way ANOVA with Bonferroni's multiple comparisons test. Data with two groups were tested by two-sided unpaired t-test (data with normal distribution).

Results

UUO induces renal damage and apoptosis

Urinary tract obstruction led to hydronephrosis, caused by urine stasis in the renal pelvis or calyces in the kidneys (Supplementary Fig. 2). The glomerular and tubular basement membrane as well as the brush border of the proximal tubules were visualized by the periodic acid Schiff (PAS) staining. The increases in mesangial matrix deposition in the glomeruli in both WT UUO and *Trpc6*$^{-/-}$ UUO *versus* sham kidneys implicates renal damage induced by UUO (Fig. 1A and B). Besides, there were no differences in glomerular injury in WT *versus* *Trpc6*$^{-/-}$ kidneys upon UUO indicating similar glomerular damage in both genotypes (Fig. 1A and B). Next, we stained sections of the kidneys with antibodies against proliferating cell nuclear antigen (PCNA) and programmed cell death marker cleaved-caspase 3 (cCasp3). UUO-induced increases in PCNA positive (PCNA^{+}) cells and cCasp3 positive (cCasp3^{+}) cells were clearly visible in the kidneys of both WT and *Trpc6*$^{-/-}$ mice (Fig. 2A, C). Although there was no difference in the number of PCNA^{+} cells between UUO WT and *Trpc6*$^{-/-}$ kidneys (Fig. 2B), less cCasp3 positive cells were found in *Trpc6*$^{-/-}$ UUO kidneys compared to WT UUO kidneys, indicating that ureteral obstructed *Trpc6*$^{-/-}$ kidneys show less apoptosis compared to obstructed WT kidneys (Fig. 2D).

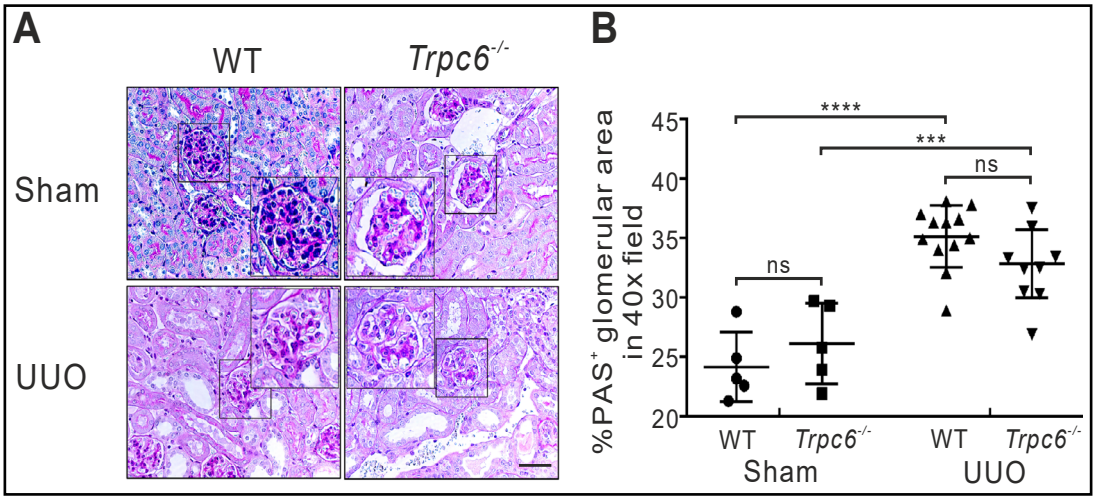

Fig. 1. PAS stained kidneys. (A): Kidneys stained with the periodic acid Schiff (PAS) stain to detect glomerular damage. (B) Quantification of the PAS positive areas in the kidneys. All images were taken at a magnification of 40x. Scale bar: 50 µm. All values are means ± SD. ns p>0.05, ***p<0.001 and ****p<0.0001. Wild type (WT) and *Trpc6*$^{-/-}$ sham groups included n=5 kidney samples each. WT and *Trpc6*$^{-/-}$ UUO-treated groups encompassed n=12 (WT) and n=11 (*Trpc6*$^{-/-}$) kidney samples. ns, not significant.

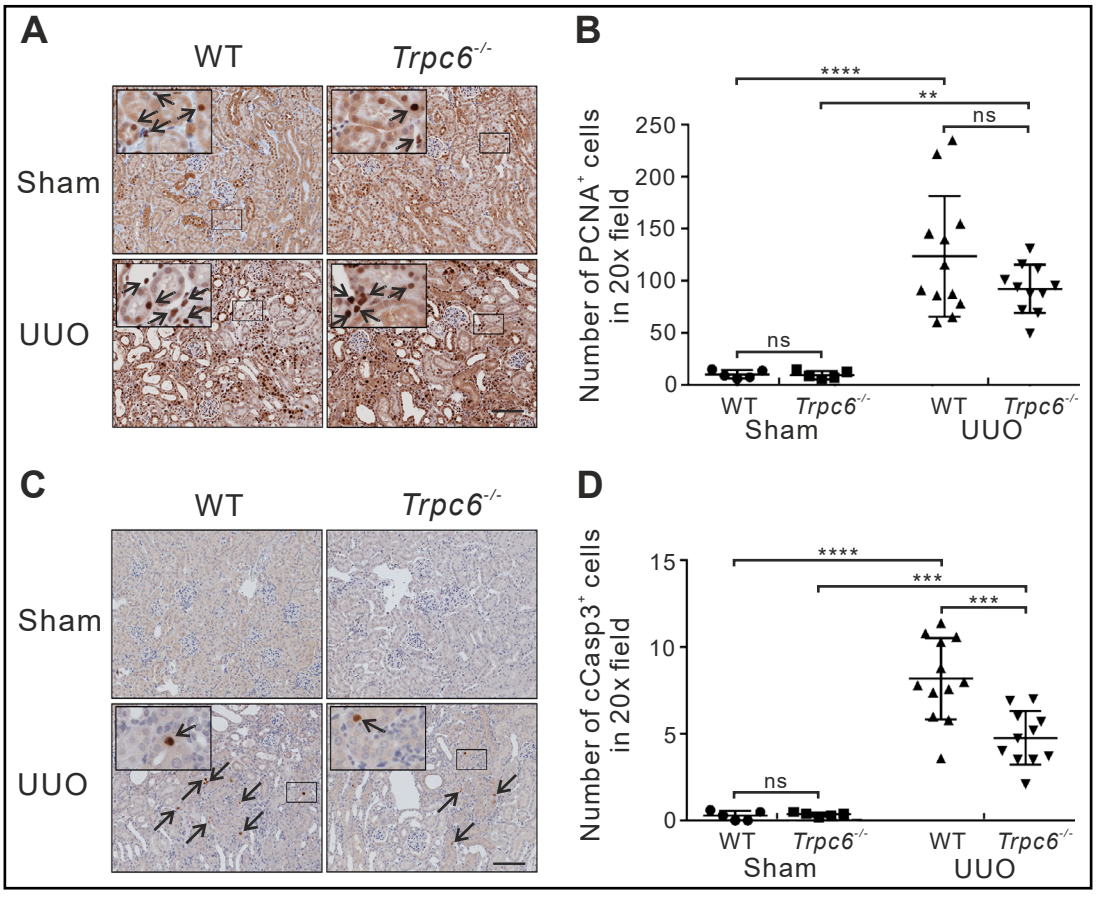

Fig. 2. Markers of proliferation and apoptosis. (A) Proliferating cell nuclear antigen (PCNA) antibody staining: marker of cell regeneration. Arrows show positive cells. All images were taken at a magnification of 20x. Scale bar: 100 µm. (B) Quantification of renal cells positively stained for PCNA. (C) Cleaved-caspase 3 (cCasp3) antibody staining: marker of apoptosis. Arrows show positive cells. All images were taken at a magnification of 20x. Scale bar: 100 µm. (D) Quantification of renal cells positively stained for cCasp3. All values are means ± SD. ns p>0.05, ***p<0.001 and ****p<0.0001. Wild type (WT) and *Trpc6*$^{-/-}$ sham groups included n=5 kidney samples each. WT and *Trpc6*$^{-/-}$ UUO-treated groups encompassed n=12 (WT) and n=11 (*Trpc6*$^{-/-}$) kidney samples. ns, not significant.

Role of TRPC6-deficiency in renal inflammation

UUO induces immune responses such as infiltration of blood cells leading to renal inflammation [4]). Therefore, we determined whether *Trpc6*-deletion can affect renal immune infiltration as well as mRNA expression of pro-inflammatory markers in the kidneys. Antibodies against the macrophage marker F4/80 and the T-cell marker CD3 were applied in IHC analyses. UUO caused immune cell infiltration in WT and *Trpc6*$^{-/-}$ kidneys, as assessed by F4/80 positive (F4/80^{+}) areas and the numbers of CD3 positive (CD3^{+}) cells in the respective kidney sections (Fig. 3A-D). However, cellular infiltration was smaller in *Trcp6*$^{-/-}$ UUO kidneys compared to WT UUO kidneys (Fig. 3A-D) which indicates a protective effect when TRPC6 is absent.

Next, we applied qRT-PCR to analyse mRNA expression of the pro-inflammatory markers interleukin 1 beta (IL1β), interleukin 6 (IL6) and tumor necrosis factor alpha (TNFα). We found that all mentioned markers were significantly increased upon UUO in the renal cortex of both WT and *Trpc6*$^{-/-}$ kidneys (Fig. 4). Surprisingly no differences between *Trpc6*$^{-/-}$ UUO and WT UUO kidneys were seen (Fig. 4A-C).

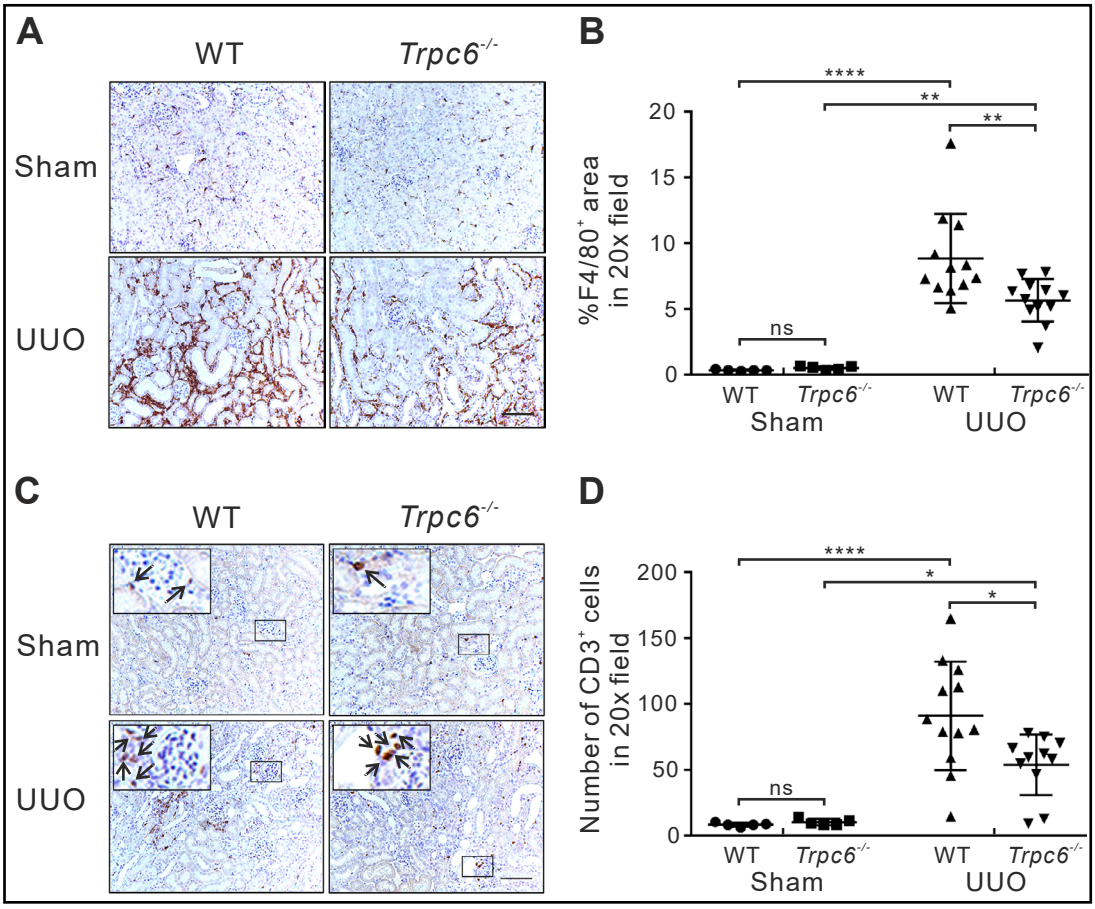

Fig. 3. Markers of inflammation in wild-type (WT) and *Trpc6*$^{-/-}$ kidneys. (A) F4/80 antibody staining: macrophage marker. (B) Quantification of the F4/80 positive areas. (C) CD3 antibody staining: T-cell marker. Arrows show positive cells (D) Quantification of the CD3 positive cells. WT and *Trpc6*$^{-/-}$ UUO-treated groups encompassed n=12 (WT) and n=11 (*Trpc6*$^{-/-}$) kidney samples. All quantification data are means ± SD. ns p>0.05, *p<0.05, **p<0.01 and ****p<0.0001. WT and *Trpc6*$^{-/-}$ sham groups included n=5 kidney samples each. All images were taken at a magnification of 20x. Scale bar: 100 µm. ns, not significant.

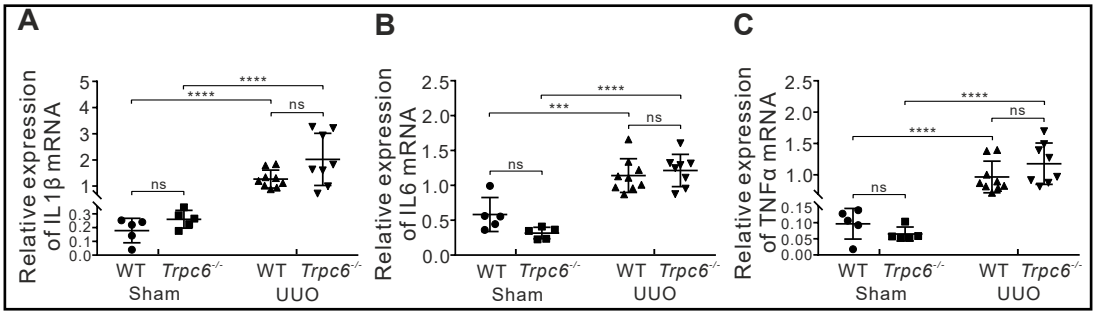

Fig. 4. Expression of inflammatory markers in wild-type (WT) and *Trpc6*$^{-/-}$ kidneys. Renal mRNA levels of (A) interleukin 1 beta (IL1β), (B) interleukin 6 (IL6) and (C) tumor necrosis factor alpha (TNFα) in sham-operated groups and in UUO-operated groups. Renal mRNA expression data were determined in n=5 each for sham-operated WT and *Trpc6*$^{-/-}$ kidneys, n=9 for UUO-operated WT kidneys and n=8 for UUO-operated *Trpc6*$^{-/-}$ kidneys. The relative standard curve method was used for relative quantification. All data are means ± SD, ns p>0.05, ***p<0.001, ****p<0.0001. ns, not significant.

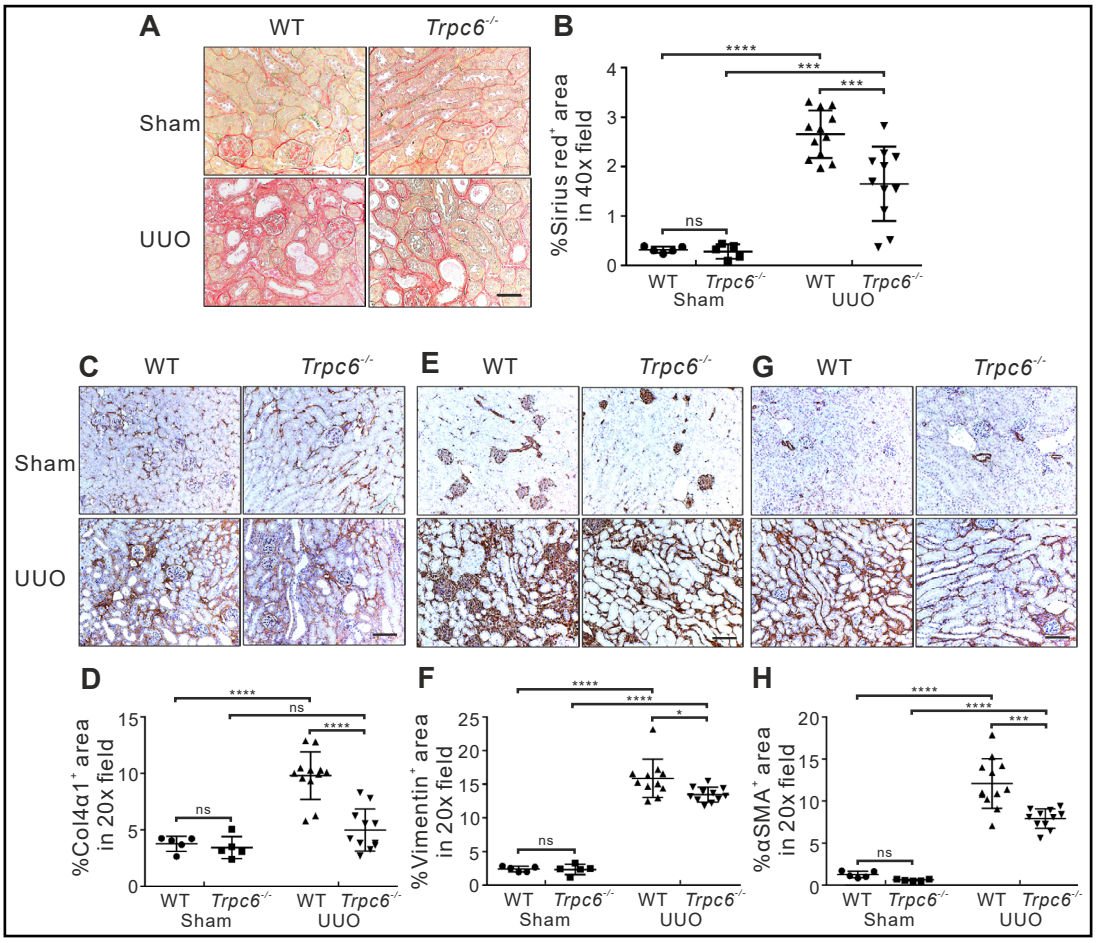

Fig. 5. Expression of fibrosis markers. (A) Sirius red (SR) staining (40x, Scale bar: 50 µm). (B) Quantification of the SR positive areas. (C) Collagen type 4, alpha 1 (Col4α1) antibody staining: fibrosis marker (20x, Scale bar: 100 µm). (D) Quantification of the Col4α1 positive areas. (E) Vimentin antibody staining: mesenchymal marker (20x, Scale bar: 100 µm. (F) Quantification of the vimentin positive areas. (G) Alpha smooth muscle actin (αSMA) antibody staining: myofibroblast marker (20x, Scale bar: 100 µm). (H) Quantification of the αSMA positive areas. Wild type (WT) and *Trpc6*$^{-/-}$ sham groups included n=5 kidney samples each. WT and *Trpc6*$^{-/-}$ UUO-treated groups encompassed n=12 (WT) and n=11 (*Trpc6*$^{-/-}$) kidney samples. All quantification data are means ± SD. ns p>0.05, *p<0.05, ***p<0.001 and ****p<0.0001. ns, not significant.

Role of TRPC6-deficiency in renal fibrosis

To examine a possible role of TRPC6-deficiency in renal fibrosis, we performed histological analysis including IHC and measured gene expression by qRT-PCR. A *Sirius red* (SR) stain was performed and SR positive (SR$^+$) areas were quantified (Fig. 5A, B) to assess the degree of collagen deposition in the kidneys. Sham-treated kidneys of either genotype exhibited only small areas of SR$^+$ areas (Fig. 5A). In contrast, WT UUO kidneys displayed a 6-fold increase in SR$^+$ areas compared to controls. This increase in collagen deposition was smaller in *Trpc6*$^{-/-}$ UUO kidneys compared to WT UUO kidneys (Fig. 5B). Next, IHC studies were performed using antibodies against collagen type 4 alpha 1 (Col4α1) to determine the level of fibrosis, the mesenchymal marker vimentin to identify epithelial-to-mesenchymal transition (EMT) of tubular epithelial cells and alpha smooth muscle actin (αSMA) to detect myofibroblasts and mesangial cells as indicators of cell types involved in fibrosis (Fig. 5C-H). We observed a significant increase in Col4α1 positive (Col4α1$^+$) area in UUO kidneys compared to sham kidneys of both genotypes (Fig. 5C, D). However, this increase in Col4α1 positive (Col4α1$^+$) area was smaller in *Trpc6*$^{-/-}$ UUO kidneys compared to WT UUO kidneys

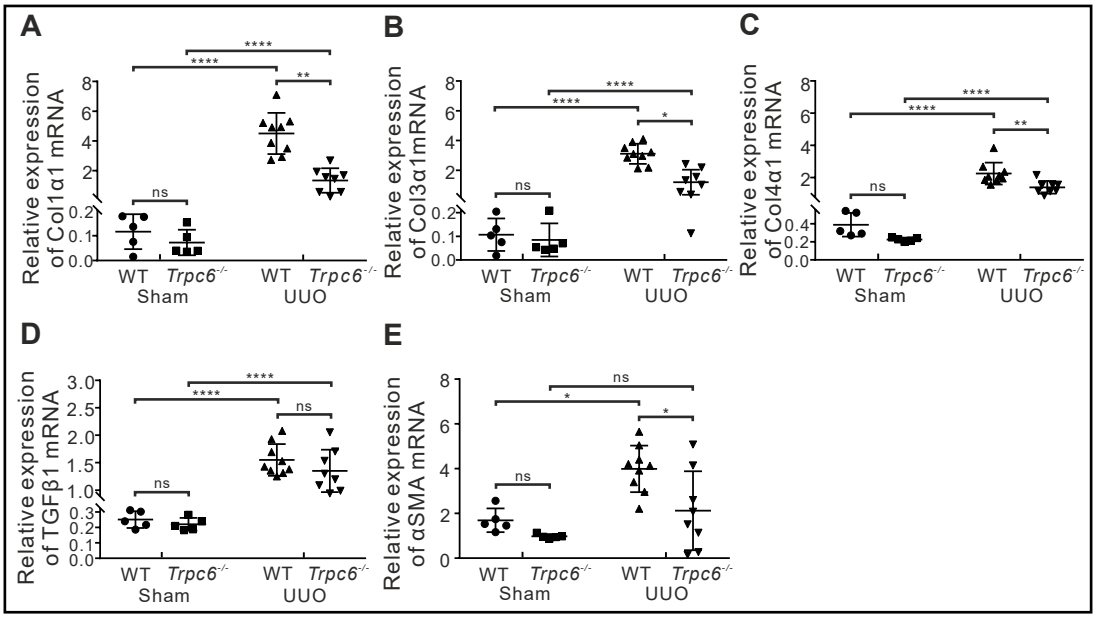

Fig. 6. Expression of genes involved in renal fibrosis in kidneys of wild-type (WT) and *Trpc6*$^{-/-}$ mice. Renal mRNA levels of (A) collagen type 1, alpha1 (Col1α1), (B) collagen type 3, alpha1 (Col3α1), (C) collagen type 4, alpha1 (Col4α1), (D) transforming growth factor beta 1 (TGFβ1) and (E) alpha smooth muscle actin (αSMA) in sham-operated groups and in UUO-operated groups. Renal mRNA expression data were determined in n=5 each for sham-operated WT and *Trpc6*$^{-/-}$ mice, n=9 for UUO-operated WT mice and n=8 for UUO-operated *Trpc6*$^{-/-}$ mice. The relative standard curve method was used for relative quantification. All data are means ± SD., ns p>0.05, *p<0.05, **p<0.01, ***p<0.001, ****p<0.0001. ns, not significant.

(Fig. 5C, D). Furthermore, a marked increase in vimentin positive (vimentin^{+}) area (Fig. 5E, F) and αSMA positive (αSMA^{+}) area (Fig. 5G, H) was observed in UUO kidneys of both genotypes. Again, the increase in vimentin^{+} mesenchymal cells and αSMA^{+} myofibroblasts was smaller in *Trpc6*$^{-/-}$ UUO kidneys compared to WT UUO kidneys (Fig. 5E-H). Taken together, these data suggest a protective effect in renal fibrosis when TRPC6 is absent.

By using qRT-PCR, we analysed the mRNA expression of pro-fibrotic markers in renal cortex, including collagen type 1 alpha 1 (Col1α1), collagen type 3 alpha 1 (Col3α1), collagen type 4 alpha 1 (Col4α1), transforming growth factor beta 1 (TGFβ1) and αSMA (Fig. 6). Whereas UUO caused increased mRNA expression of all pro-fibrotic markers in the renal cortex of WT mice (Fig. 6A-E), *Trpc6*-deficiency UUO kidneys displayed only a significant increase in Col3α1, Col4α1 and TGFβ1 but not αSMA mRNA levels (Fig. 6B, C, D). When we compared the mRNA expression of the aforementioned markers within the UUO-treated groups, we found that all pro-fibrotic markers except for TGFβ1 were reduced in *Trcp6*$^{-/-}$ UUO kidneys relative to WT UUO kidneys (Fig. 6A-E) supporting the idea that *Trpc6*-deficiency is protective in this kidney disease model.

Expression profile of TRPC channels in renal cortex

The genomic absence of one TRPC channel may affect the expression of the remaining which could contribute to the renal outcome. We performed qRT-PCR to first identify the relative expression of TRPC family members (TRPC1-7) in renal cortices of WT and *Trpc6*-deficient mice. In sham-operated kidneys we found that deletion of *Trpc6* was associated with reduced *Trpc2*, *Trpc3* and *Trpc4* mRNA expression compared to WT kidneys (Fig. 7A-D). Conversely, *Trpc6*-deficiency increased *Trpc1* mRNA expression. Similarly, *Trpc5* mRNA was present in *Trpc6*$^{-/-}$ kidneys but below detection limit in WT kidneys (Fig. 7E). As reported earlier [18], whereas *Trpc6* mRNA expression could be determined in WT kidneys it was below the detection levels in *Trpc6*$^{-/-}$ kidneys (Fig. 7F). *Trpc7* mRNA was not detectable in

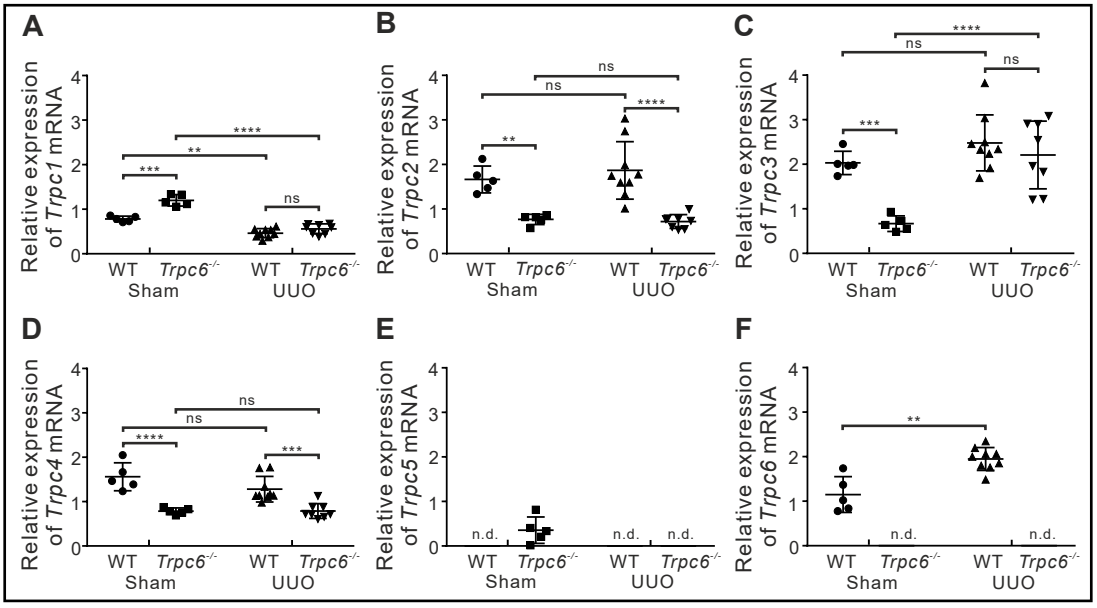

Fig. 7. Expression of renal TRPC channels in wild-type (WT) and *Trpc6*$^{-/-}$ mice. Renal mRNA levels of (A) transient receptor potential cation channel 1 (TRPC1), (B) TRPC2 (C) TRPC3 (D) TRPC4 (E) TRPC5 and (F) TRPC6 in sham-operated groups and in UUO-operated groups. Renal mRNA expression data were determined in n=5 each for sham-operated WT and *Trpc6*$^{-/-}$ mice, n=9 for UUO-operated WT mice and n=8 for UUO-operated *Trpc6*$^{-/-}$ mice. The relative standard curve method was used for relative quantification. All data are means ± SD., ns p>0.05, **p<0.01, ***p<0.001, ****p<0.0001. ns, not significant; n.d., not detected.

both WT and *Trpc6*$^{-/-}$ kidneys, but was present in WT brain tissue, which served as positive control (Supplementary Fig. 3B).

Next, we determined in WT animals whether the relative expression of TRPC isoforms is affected by UUO. Interestingly, ureter obstruction did not affect the relative mRNA expression levels of most TRPC family members including *Trpc2*, *Trpc3*, *Trpc4*, and *Trpc5* (Fig. 7B-E). In contrast UUO provoked an approximately 50% downregulation of *Trpc1* and notably a 60% upregulation of *Trpc6* mRNA expression in WT kidneys (Fig. 7A and F) relative to sham-operated WT animals.

On the other hand, *Trpc6*-deficiency provoked a highly significant decrease of *Trpc2* and *Trpc4* transcript levels in both sham and UUO kidneys (Fig. 7B, D) whereas *Trpc1* and *Trpc3* mRNA levels showed significant differences under sham conditions compared to WT (Fig. 7A, C), in UUO kidneys their level was similar. In addition, *Trpc5* transcript levels were below detection levels in the presence and absence of *Trpc6* (Fig. 7E), and as expected in *Trpc6*$^{-/-}$ kidneys lacking *Trpc6* mRNA (Fig. 7F).

UUO in NZO mice

We next used the complex disease NZO mouse model to evaluate UUO nephropathy and regulation of TRPC channel expression in an inbred obese mouse strain carrying susceptibility genes for diabetes and hypertension. In NZO mice, UUO caused also significant damage to the kidney. Histological analyses showed that UUO induced increases in PAS^{+} area, PCNA^{+} cells, SR^{+} area, F4/80^{+} area and CD3^{+} cells (Fig. 8). Furthermore, we detected an UUO-induced increase in mRNA expression of the pro-fibrotic markers Col1α1, Col3α1, Col4α1 and TGFβ1 (Fig. 9A) and the pro-inflammatory markers IL1β, IL6, TNFα, ICAM1, VCAM1 and MCP1 relative to the sham-operated group (Fig. 9B).

We also examined the relative expression profile of TRPC genes in kidneys of NZO mice in sham and UUO kidneys by qRT-PCR. NZO sham kidneys expressed mRNA of six TRPC genes in renal cortex (Fig. 10). UUO caused, similarly to the previous findings in WT mice, up-regulation of *Trpc6* mRNA expression while *Trpc1* and *Trpc5* mRNA expression was

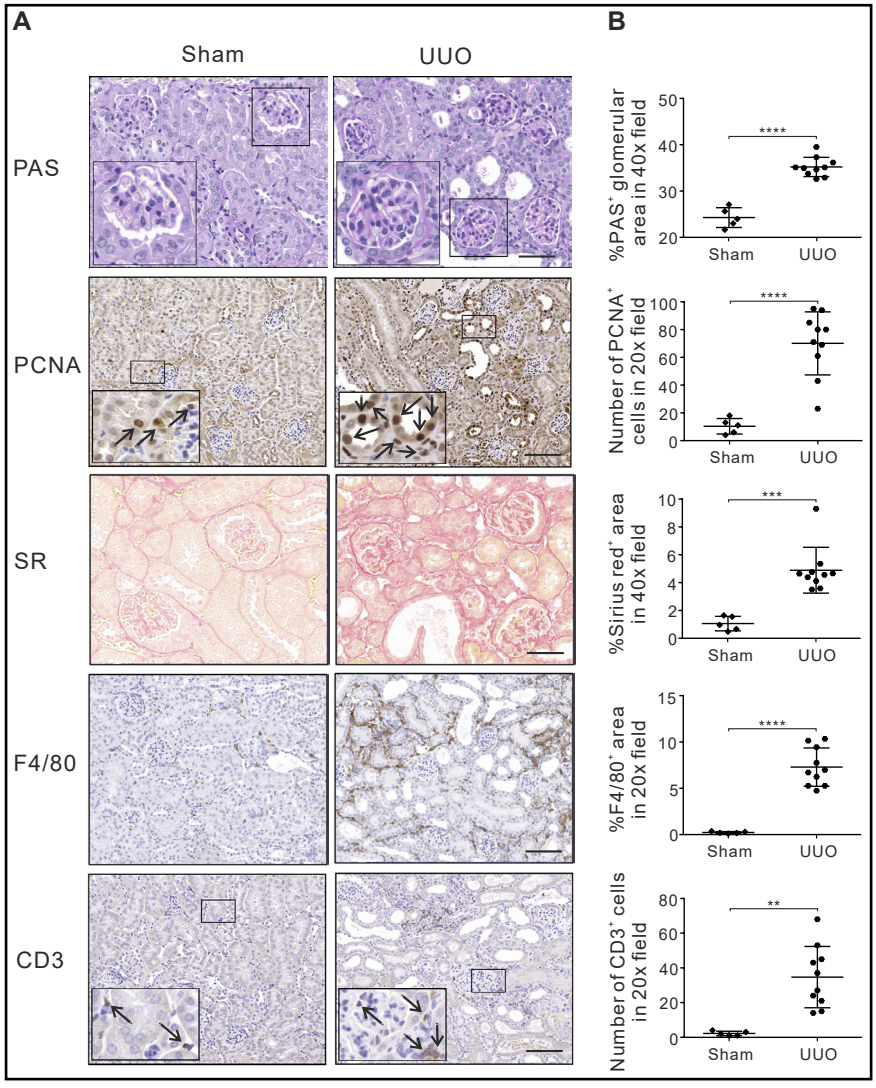

Fig. 8. Markers of fibrosis and inflammation in New Zealand obese (NZO) mice. (A) Periodic acid Schiff (PAS) stain: marker of glomerular damage (40x). Scale bar: 50 µm. Proliferating cell nuclear antigen (PCNA) antibody stain: marker of cell regeneration (20x. Scale bar: 100 µm; arrows show positive cells). Sirius red (SR) stain: marker of interstitial fibrosis (40x. Scale bar: 50 µm). F4/80 antibody stain: macrophage marker (20x. Scale bar: 100 µm) and CD3 antibody stain: T-cell marker (20x. Scale bar: 100 µm; arrows show positive cells) in sham-operated group and UUO-operated groups. (B) All quantification data are means ± SD. Data were determined in n=5 for sham-operated kidneys, n=10 for UUO-operated kidneys. **p<0.01, ***p<0.001 and ****p<0.0001.

down-regulated. There was no change in *Trpc2* and *Trpc3* mRNA expression in NZO kidneys upon UUO surgery (Fig. 10). Noteworthy, *Trpc7* mRNA was not detectable in NZO kidneys without and in response to UUO (Fig. 10), which is in line with our findings in WT and *Trpc6*$^{-/-}$ kidneys (Supplementary Fig. 3).

Discussion

Renal fibrosis and inflammation

Mechanisms that promote kidney disease progression include renal atrophy, fibrosis and increased leukocyte infiltration into the kidneys [33, 34]. Renal fibrosis and inflammation are two histological hallmarks of progressive kidney disease and specific antibody staining is a common tool to estimate renal damage [35, 36]. UUO is an established model for renal fibrosis and chronic kidney failure [4]. TRPC6, which is regarded a major slit diaphragm-associated channel, can be increasingly detected in various kidney diseases such as FSGS [37, 38], diabetic nephropathy [22, 39-41], minimal change nephrosis [38, 42] and membranous nephropathy

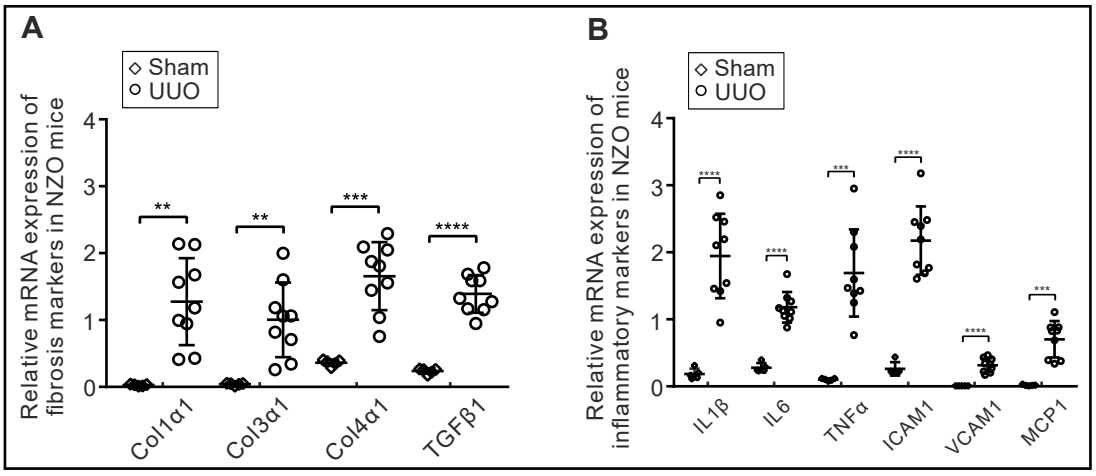

Fig. 9. Expression of markers of fibrosis and inflammation in New Zealand obese (NZO) mice. (A) Renal mRNA levels of fibrosis markers: collagen type 1, alpha 1 (Col1α1), collagen type 3, alpha 1 (Col3α1), collagen type 4, alpha 1 (Col4α1) and transforming growth factor beta 1 (TGFβ1) in sham-operated group and in UUO-operated group. (B) Renal mRNA levels of inflammation markers: interleukin 1 beta (IL1β), interleukin 6 (IL6), tumor necrosis factor alpha (TNFα), intercellular adhesion molecule 1 (ICAM1), vascular cell adhesion molecule 1 (VCAM1) and monocyte chemotactic protein 1 (MCP1) in sham-operated group and UUO-operated groups. All mRNA expression data are determined in n=5 for sham-operated kidneys, n=9 for UUO-operated kidneys. The relative standard curve method was used for relative quantification. All data are means ± SD., **p<0.01, ***p<0.001, ****p<0.0001 and ****p<0.0001.

[42-44]. In previous studies, TRPC6 was reported to contribute to fibroblast-to-myofibroblast transdifferentiation (FMT) and is thought to promote tissue scarring [45-47]. Some study suggest that TRPC6 as a non-selective cation channel can be responsible for increased Ca^{2+} flux in myo-/fibroblasts [48]. Recent studies show that TRPC6 is involved in the pathogenesis of kidney fibrosis and genomic inhibition of the channel can reduce rat kidney fibroblast proliferation and myofibroblast differentiation *in vitro* [49]. As our study was undergoing, Wu, et al [18]. reported that inhibition of TRPC6 can ameliorate renal fibrosis in the mice based on UUO model. In the present study, we used *Trpc6*$^{-/-}$ mice and equally carried out UUO surgery to induce early stage CKD. We found similarly to Wu et al. that *Trpc6* loss reduces renal fibrosis in the murine UUO model. In addition, we were able to show that TRPC6-deficiency caused a decreased mRNA expression of multiple pro-fibrotic genes. Our results therefore confirm the previous finding that *Trpc6* deletion attenuates UUO-induced kidney fibrosis in mice [18].

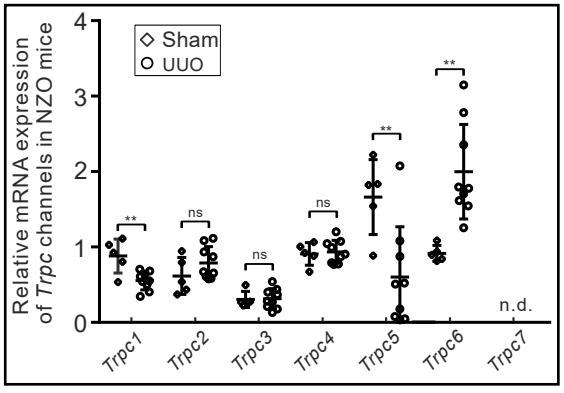

Fig. 10. Expression of renal TRPC channels in New Zealand obese (NZO) mice. Renal mRNA levels of TRPC1-7 channels in sham-operated group and in UUO-operated group. Renal mRNA expression data were determined in n=5 sham-operated kidneys, n=9 UUO-operated kidneys. The relative standard curve method was used for relative quantification. All data are means ± SD, ns p>0.05, **p<0.01, ns: not significant. n.d.: not detected.

The renal damage occurring in CKD is, at least in part, promoted by the immune system [50]. Most kidney diseases involve an accumulation of immune cells of the innate (e.g. macrophages and neutrophils) and adaptive (e.g. T-cells) immune system. In particular, tubulointerstitial monocyte immune infiltration can mediate tissue remodeling that

ultimately promotes fibrogenesis, renal atrophy and thus, kidney failure [51-53]. Our results revealed a less infiltration of CD3 cells and F4/80$^+$ area in UUO *Trpc6*$^{-/-}$ kidneys compared to those in UUO WT kidneys. We have therefore performed qPCR analysis in our model as well to quantify inflammatory cytokine levels. Whereas, UUO provoked an increase in mRNA expression of the pro-inflammatory markers in both *Trpc6*$^{-/-}$ and WT kidneys we did not find a significant beneficial effect of lacking *Trpc6* on the expression of pro-inflammatory markers at the mRNA level upon UUO surgery. This might be because we collected tissues only at day 7 after induction of UUO and therefore we might have missed the time-point where lacking *Trpc6* influence pro-inflammatory gene expression. On the other side it lacking *Trpc6* can influence immune cell function and therefore pro-inflammatory cytokine expression [54]. Taken together, our data point to a complex (in-)direct contribution of TRPC6 to renal inflammation in the UUO model.

To estimate renal apoptosis as well as regenerative potential, kidney sections were stained with antibodies against the apoptosis marker cleaved-caspase 3 (cCasp3) and the mitosis marker proliferating cell nuclear antigen (PCNA). Since cCasp3 and PCNA levels correlate positively with renal injury, they are commonly used to determine the degree of renal damage under chronic damaging conditions [55-57]. It is known that chronic activation of TRPC6 is positively correlated with the rate of apoptosis in cells such as podocytes [58, 59] and endothelial cells [60]. Indeed, we found less cCasp3 positive cells in kidneys of *Trpc6*$^{-/-}$ mice underwent UUO. It might however reflect the less inflammatory cell infiltration, since cCasp positive cells were count in the whole kidney section irrespective of the signal's origin. PCNA is known as a probe for the detection of cell proliferative activity [61]. In our study, PCNA$^+$ cells were found to be increased after UUO in both WT and *Trpc6*$^{-/-}$ kidneys. Nevertheless, we did not find significant difference in PCNA$^+$ cells between WT and *Trpc6*$^{-/-}$ mice. Correlated with the result of cCasp3 cell infiltration, it might be due to an imbalance between cell apoptosis and proliferative activity, or it might be because PCNA is also regulated by other factors, e.g. p53[62] and DNA damage binding protein 2 (DDB2) [63]. In summary, the results indicate that TRPC6-deficiency protects renal cells from UUO-induced apoptosis.

In summary – based on our key findings of reduced renal fibrosis and inflammation after UUO in the *Trpc6*$^{-/-}$ mice, we believe that these changes are associated with improved kidney function, which ultimately should delay CKD progression to end stage renal disease. Therefore, we suggest that non-cell specific TRPC6 inhibition seems to be meaningful therapeutic approach to improve the outcome of CKD. However, further studies are needed to evaluate this approach in other experimental models of CKD.

TRPC6 and other TRPCs

We further revealed that TRPC6-deficiency *per se* impacts on renal TRPC channel expression in mice as indicated by reduced mRNA expression of TRPC2, TRPC3 and TRPC4 and increased mRNA expression of TRPC1. Moreover, we found that UUO caused reduced *Trpc1* mRNA and increased *Trpc6* mRNA expression without changes of *Trpc3* expression in WT kidneys. Collectively, the data suggest that counterbalanced or increased expression of TRPC1 and TRPC6 could play a role in UUO-induced kidney damage. Since genomic deletion of *Trpc6* improved renal fibrosis and was associated with an increase of *Trpc1* mRNA expression and a reduction of *Trpc2, Trpc3* and *Trpc4* mRNA expression in sham-operated kidneys to levels similar or greater than those observed in UUO kidneys, we conclude that TRPC6 could drive renal fibrosis with or without modifying effects of TRPC1/2/3/4. Our studies revealed an unrecognized renal counter-regulation of TRPC5 and TRPC7 gene expression. This conclusion is supported by findings that TRPC5 and TRPC7 is not expressed in normal kidneys of mice [64].

Of note, the data in the present study shows that the deficiency for TRPC6 is associated with reduced *Trpc3* mRNA expression in *Trpc6*$^{-/-}$ kidneys compared to WT kidneys, which disappears in obstructive nephropathy. At a first glance, this is surprising as we observed in our previous studies on *Trpc6*$^{-/-}$ mice that loss of TRPC6 is associated with up-regulation of

constitutively active TRPC3-type channels in some arteries [27]. However, to our knowledge, TRPC channels (TRPC1-7) expression and resulting putative (functional) counterbalancing effects have not been investigated in experimental obstructive nephropathy. This is of particular interest for TRPC3, which is capable of contributing to fibrogenesis and tissue inflammation [65-69]. Additionally, Wu et al. reported that TRPC3 mRNA expression is upregulated in UUO-induced renal fibrosis [18]. However, we could not detect an increase in TRPC3 expression level in WT kidneys (neither in our NZO mouse model) which argues against an important role in progression of fibrosis in obstructive nephropathy. Based on our findings, it is unlikely that increased TRPC3 expression upon UUO accounts for the beneficial role of TRPC6-deficiency in this model of kidney failure. These mechanisms might be particularity relevant for inherited FSGS caused by mutations in TRPC6 [6, 70]. This conclusion is supported by recent findings demonstrating that knockout of both TRPC3 and TRPC6 did not diminish UUO-induced fibrosis more than deletion of TRPC6 alone [18]. BTP2, an inhibitor of several TRPC channels, including TRPC3 and TRPC6, had an effect similar to that of *Trpc6* knockout on fibrosis, but also attenuated the up-regulation of TRPC6 expression, suggesting that TRPC6 channel activity may induce its own gene expression in the UUO model [2] and promote fibrosis in this model. Nevertheless, future studies using more specific TRPC3/6 blockers are necessary to clarify the contribution of TRPC3 in the absence and presence of functional TRPC6 channels. Recently, novel TRPC6 blockers have been developed [71-73], which could represent important tools to evaluate the role of TRPC6 in these conditions.

Diabetic nephropathy

Today, 25-40% of diabetic patients suffer from diabetic nephropathy [74, 75]. Thus, diabetic patients can be considered as high-risk patients for the development of chronic kidney disease. Diabetic nephropathy shows pronounced glomerular changes that are present in patients with long-standing diabetes often even before the detection of albumin in the urine. Several mechanisms that can lead to diabetic nephropathy are under discussion. We evaluated whether UUO-operated NZO mouse model could represent a model of progressive nephropathy in co-morbid conditions of obesity, hypertension and type 2 diabetes [24], which had not been reported before. Our study shows that UUO can successfully induce renal fibrosis and inflammatory infiltration in the NZO mouse model (NZO/HIBomDife) carrying susceptibility genes for obesity, diabetes and hypertension.

More importantly, our study also suggests that *Trpc1-4 and Trpc6* expression in NZO mice underwent UUO/sham-operation showed similar tendency to those observed in WT mice, which verified the regulation of TRPC channels in a second mouse model. Interestingly, we found that *Trpc5* expression was detected in the kidneys of NZO mice, which indicated that TRPC5 could be specifically involved in this process in NZO mice. Our results suggest that the UUO-operated NZO mouse model might represent a valuable mouse model to be used to evaluate the specific contribution of TRPC6 and other TRPC channel subfamilies in the renal injury upon obesity, hypertension and diabetes. This approach could take advance of testing better, i.e. TRPC subfamily specific blockers and agonists. In spite of recent progress in this field [71-73, 76], we are optimistic that those drugs are becoming available in the near future for *in vivo* testing.

Conclusion

Our study observed that inhibition of TRPC6 is associated with a decrease in inflammatory cell infiltration in murine UUO model for the first time. Also, the findings are in line with the concept that up-regulation of TRPC6 contributes to fibrosis in UUO kidneys. The results support the view that increased TRPC6 expression can play an important pathophysiological role in the development of progressive kidney disease [14, 38, 77, 78]. Moreover, the present results imply that the genomic loss of TRPC6 is associated with dysregulation of multiple

TRPC channels (TRPC1-4) under chronic kidney damaging conditions, which could represent additional drivers of renal fibrosis and chronic kidney disease. Our results show that UUO causes also up-regulation of TRPC6 in kidneys of NZO mice, which implies that inhibition of TRPC6 is also a promising therapeutic strategy for treatment of renal fibrosis and immune cell infiltration in polygenic models for the human metabolic syndrome.

Acknowledgements

This work was supported by the Deutsche Forschungsgemeinschaft (DFG) (B.N. and M.G.). We thank Elisabeth Meyer, May-Britt Köhler, Juliane Anders and Jana Czychi for help and expert technical assistance. M. Gollasch and L. Markó jointly supervised this work.

All animal protocols were locally approved by Landesamt für Umwelt, Gesundheit und Verbraucherschutz (LUGV) Brandenburg, Germany (Permit-Number: 2347-7-2016).

All authors planned and designed experimental studies. W.K. and T.H. performed the experiments and analyzed the data. M.G., L.M. and S.K. contributed reagents/materials/analysis tools. W.K. and M.G. drafted the manuscript and all authors contributed to its completion. We acknowledge support from the German Research Foundation (DFG) and the Open Access Publication Fund of Charité – Universitätsmedizin Berlin.

Disclosure Statement

The authors have no conflicts of interest to declare.

References

1 Farris AB, Colvin RB: Renal interstitial fibrosis: mechanisms and evaluation. Curr Opin Nephrol Hypertens 2012;21:289-300.
2 Schlondorff J: TRPC6 and kidney disease: sclerosing more than just glomeruli? Kidney Int 2017;91:773-775.
3 Eddy AA: Overview of the cellular and molecular basis of kidney fibrosis. Kidney Int Suppl (2011) 2014;4:2-8.
4 Chevalier RL, Forbes MS, Thornhill BA: Ureteral obstruction as a model of renal interstitial fibrosis and obstructive nephropathy. Kidney Int 2009;75:1145-1152.
5 Riehle M, Tsvetkov D, Gohlke BO, Preissner R, Harteneck C, Gollasch M, Nurnberg B: Molecular basis for the sensitivity of TRP channels to polyunsaturated fatty acids. Naunyn Schmiedebergs Arch Pharmacol 2018;391:833-846.
6 Marko L, Mannaa M, Haschler TN, Kramer S, Gollasch M: Renoprotection: focus on TRPV1, TRPV4, TRPC6 and TRPM2. Acta Physiol (Oxf) 2017;219:589-612.
7 Strubing C, Krapivinsky G, Krapivinsky L, Clapham DE: TRPC1 and TRPC5 form a novel cation channel in mammalian brain. Neuron 2001;29:645-655.
8 Hofmann T, Schaefer M, Schultz G, Gudermann T: Subunit composition of mammalian transient receptor potential channels in living cells. Proc Natl Acad Sci U S A 2002;99:7461-7466.
9 Storch U, Forst AL, Philipp M, Gudermann T, Mederos y Schnitzler M: Transient receptor potential channel 1 (TRPC1) reduces calcium permeability in heteromeric channel complexes. J Biol Chem 2012;287:3530-3540.
10 Kim J, Kwak M, Jeon JP, Myeong J, Wie J, Hong C, Kim SY, Jeon JH, Kim HJ, So I: Isoform- and receptor-specific channel property of canonical transient receptor potential (TRPC)1/4 channels. Pflugers Arch 2014;466:491-504.
11 Woo JS, Lee KJ, Huang M, Cho CH, Lee EH: Heteromeric TRPC3 with TRPC1 formed via its ankyrin repeats regulates the resting cytosolic Ca2+ levels in skeletal muscle. Biochem Biophys Res Commun 2014;446:454-459.

12 Rubaiy HN, Ludlow MJ, Henrot M, Gaunt HJ, Miteva K, Cheung SY, Tanahashi Y, Hamzah N, Musialowski KE, Blythe NM, Appleby HL, Bailey MA, McKeown L, Taylor R, Foster R, Waldmann H, Nussbaumer P, Christmann M, Bon RS, Muraki K, et al.: Picomolar, selective, and subtype-specific small-molecule inhibition of TRPC1/4/5 channels. J Biol Chem 2017;292:8158-8173.
13 Ma R, Chaudhari S, Li W: Canonical Transient Receptor Potential 6 Channel: A New Target of Reactive Oxygen Species in Renal Physiology and Pathology. Antioxid Redox Signal 2016;25:732-748.
14 Ilatovskaya DV, Staruschenko A: TRPC6 channel as an emerging determinant of the podocyte injury susceptibility in kidney diseases. Am J Physiol Renal Physiol 2015;309:F393-397.
15 Dogra S, Kaskel F: Steroid-resistant nephrotic syndrome: a persistent challenge for pediatric nephrology. Pediatr Nephrol 2017;32:965-974.
16 Ilatovskaya DV, Palygin O, Chubinskiy-Nadezhdin V, Negulyaev YA, Ma R, Birnbaumer L, Staruschenko A: Angiotensin II has acute effects on TRPC6 channels in podocytes of freshly isolated glomeruli. Kidney Int 2014;86:506-514.
17 Huang H, You Y, Lin X, Tang C, Gu X, Huang M, Qin Y, Tan J, Huang F: Inhibition of TRPC6 Signal Pathway Alleviates Podocyte Injury Induced by TGF-beta1. Cell Physiol Biochem 2017;41:163-172.
18 Wu YL, Xie J, An SW, Oliver N, Barrezueta NX, Lin MH, Birnbaumer L, Huang CL: Inhibition of TRPC6 channels ameliorates renal fibrosis and contributes to renal protection by soluble klotho. Kidney Int 2017;91:830-841.
19 Zhang D, Freedman BI, Flekac M, Santos E, Hicks PJ, Bowden DW, Efendic S, Brismar K, Gu HF: Evaluation of genetic association and expression reduction of TRPC1 in the development of diabetic nephropathy. Am J Nephrol 2009;29:244-251.
20 Graham S, Gorin Y, Abboud HE, Ding M, Lee DY, Shi H, Ding Y, Ma R: Abundance of TRPC6 protein in glomerular mesangial cells is decreased by ROS and PKC in diabetes. Am J Physiol Cell Physiol 2011;301:C304-315.
21 Zhang X, Song Z, Guo Y, Zhou M: The novel role of TRPC6 in vitamin D ameliorating podocyte injury in STZ-induced diabetic rats. Mol Cell Biochem 2015;399:155-165.
22 Ma R, Liu L, Jiang W, Yu Y, Song H: FK506 ameliorates podocyte injury in type 2 diabetic nephropathy by down-regulating TRPC6 and NFAT expression. Int J Clin Exp Pathol 2015;8:14063-14074.
23 Fesus G, Dubrovska G, Gorzelniak K, Kluge R, Huang Y, Luft FC, Gollasch M: Adiponectin is a novel humoral vasodilator. Cardiovasc Res 2007;75:719-727.
24 Mirhashemi F, Scherneck S, Kluth O, Kaiser D, Vogel H, Kluge R, Schurmann A, Neschen S, Joost HG: Diet dependence of diabetes in the New Zealand Obese (NZO) mouse: total fat, but not fat quality or sucrose accelerates and aggravates diabetes. Exp Clin Endocrinol Diabetes 2011;119:167-171.
25 Zavaritskaya O, Zhuravleva N, Schleifenbaum J, Gloe T, Devermann L, Kluge R, Mladenov M, Frey M, Gagov H, Fesus G, Gollasch M, Schubert R: Role of KCNQ channels in skeletal muscle arteries and periadventitial vascular dysfunction. Hypertension 2013;61:151-159.
26 Joost HG, Schurmann A: The genetic basis of obesity-associated type 2 diabetes (diabesity) in polygenic mouse models. Mamm Genome 2014;25:401-412.
27 Dietrich A, Mederos YSM, Gollasch M, Gross V, Storch U, Dubrovska G, Obst M, Yildirim E, Salanova B, Kalwa H, Essin K, Pinkenburg O, Luft FC, Gudermann T, Birnbaumer L: Increased vascular smooth muscle contractility in *TRPC6-/-* mice. Mol Cell Biol 2005;25:6980-6989.
28 Ma LJ, Yang H, Gaspert A, Carlesso G, Barty MM, Davidson JM, Sheppard D, Fogo AB: Transforming growth factor-beta-dependent and -independent pathways of induction of tubulointerstitial fibrosis in beta6(-/-) mice. Am J Pathol 2003;163:1261-1273.
29 Federation for Laboratory Animal Science Associations: Guidelines - Recommendations - Felasa. URL: http://www.felasa.eu/recommendations/guidelines/.
30 Gesellschaft für Versuchstierkunde: GV-SOLAS. URL: http://www.gv-solas.de/index.php?id=7.
31 American Physiological Society: Guiding Principles for the Care and Use of Vertebrate Animals in Research and Training. URL: http://www.the-aps.org/mm/SciencePolicy/About/Policy-Statements/Guiding-Principles.html.
32 Marko L, Vigolo E, Hinze C, Park JK, Roel G, Balogh A, Choi M, Wubken A, Cording J, Blasig IE, Luft FC, Scheidereit C, Schmidt-Ott KM, Schmidt-Ullrich R, Muller DN: Tubular Epithelial NF-kappaB Activity Regulates Ischemic AKI. J Am Soc Nephrol 2016;27:2658-2669.
33 Wilson DR: Renal function during and following obstruction. Annu Rev Med 1977;28:329-339.

34 Capelouto CC, Saltzman B: The pathophysiology of ureteral obstruction. J Endourol 1993;7:93-103.
35 Strutz F, Zeisberg M: Renal fibroblasts and myofibroblasts in chronic kidney disease. J Am Soc Nephrol 2006;17:2992-2998.
36 Kawakami T, Mimura I, Shoji K, Tanaka T, Nangaku M: Hypoxia and fibrosis in chronic kidney disease: crossing at pericytes. Kidney Int Suppl (2011) 2014;4:107-112.
37 Winn MP, Conlon PJ, Lynn KL, Farrington MK, Creazzo T, Hawkins AF, Daskalakis N, Kwan SY, Ebersviller S, Burchette JL, Pericak-Vance MA, Howell DN, Vance JM, Rosenberg PB: A mutation in the TRPC6 cation channel causes familial focal segmental glomerulosclerosis. Science 2005;308:1801-1804.
38 Moller CC, Wei C, Altintas MM, Li J, Greka A, Ohse T, Pippin JW, Rastaldi MP, Wawersik S, Schiavi S, Henger A, Kretzler M, Shankland SJ, Reiser J: Induction of TRPC6 channel in acquired forms of proteinuric kidney disease. J Am Soc Nephrol 2007;18:29-36.
39 Sonneveld R, van der Vlag J, Baltissen MP, Verkaart SA, Wetzels JF, Berden JH, Hoenderop JG, Nijenhuis T: Glucose specifically regulates TRPC6 expression in the podocyte in an AngII-dependent manner. Am J Pathol 2014;184:1715-1726.
40 Ilatovskaya DV, Levchenko V, Lowing A, Shuyskiy LS, Palygin O, Staruschenko A: Podocyte injury in diabetic nephropathy: implications of angiotensin II-dependent activation of TRPC channels. Sci Rep 2015;5:17637.
41 Yao XM, Liu YJ, Wang YM, Wang H, Zhu BB, Liang YP, Yao WG, Yu H, Wang NS, Zhang XM, Peng W: Astragaloside IV prevents high glucose-induced podocyte apoptosis via downregulation of TRPC6 Mol Med Rep 2016;13:5149-5156.
42 Reiser J, Polu KR, Moller CC, Kenlan P, Altintas MM, Wei C, Faul C, Herbert S, Villegas I, Avila-Casado C, McGee M, Sugimoto H, Brown D, Kalluri R, Mundel P, Smith PL, Clapham DE, Pollak MR: TRPC6 is a glomerular slit diaphragm-associated channel required for normal renal function. Nat Genet 2005;37:739-744.
43 Kistler AD, Singh G, Altintas MM, Yu H, Fernandez IC, Gu C, Wilson C, Srivastava SK, Dietrich A, Walz K, Kerjaschki D, Ruiz P, Dryer S, Sever S, Dinda AK, Faul C, Reiser J: Transient receptor potential channel 6 (TRPC6) protects podocytes during complement-mediated glomerular disease. J Biol Chem 2013;288:36598-36609.
44 Hofstra JM, Coenen MJ, Schijvenaars MM, Berden JH, van der Vlag J, Hoefsloot LH, Knoers NV, Wetzels JF, Nijenhuis T: TRPC6 single nucleotide polymorphisms and progression of idiopathic membranous nephropathy. PLoS One 2014;9:e102065.
45 Davis J, Burr AR, Davis GF, Birnbaumer L, Molkentin JD: A TRPC6-dependent pathway for myofibroblast transdifferentiation and wound healing *in vivo*. Dev Cell 2012;23:705-715.
46 Hofmann K, Fiedler S, Vierkotten S, Weber J, Klee S, Jia J, Zwickenpflug W, Flockerzi V, Storch U, Yildirim AO, Gudermann T, Konigshoff M, Dietrich A: Classical transient receptor potential 6 (TRPC6) channels support myofibroblast differentiation and development of experimental pulmonary fibrosis. Biochim Biophys Acta 2017;1863:560-568.
47 Baum J, Duffy HS: Fibroblasts and myofibroblasts: what are we talking about? J Cardiovasc Pharmacol 2011;57:376-379.
48 Berridge MJ: Calcium signalling remodelling and disease. Biochem Soc Trans 2012;40:297-309.
49 Kim EY, Yazdizadeh Shotorbani P, Dryer SE: Trpc6 inactivation confers protection in a model of severe nephrosis in rats. J Mol Med (Berl) 2018;96:631-644.
50 Kurts C, Panzer U, Anders HJ, Rees AJ: The immune system and kidney disease: basic concepts and clinical implications. Nat Rev Immunol 2013;13:738-753.
51 Mannon RB, Matas AJ, Grande J, Leduc R, Connett J, Kasiske B, Cecka JM, Gaston RS, Cosio F, Gourishankar S, Halloran PF, Hunsicker L, Rush D, De KAFI: Inflammation in areas of tubular atrophy in kidney allograft biopsies: a potent predictor of allograft failure. Am J Transplant 2010;10:2066-2073.
52 Swenson-Fields KI, Vivian CJ, Salah SM, Peda JD, Davis BM, van Rooijen N, Wallace DP, Fields TA: Macrophages promote polycystic kidney disease progression. Kidney Int 2013;83:855-864.
53 Yadav B, Prasad N, Agrawal V, Jain M, Agarwal V, Jaiswal A, Bhadauria D, Sharma RK, Gupta A: T-bet-positive mononuclear cell infiltration is associated with transplant glomerulopathy and interstitial fibrosis and tubular atrophy in renal allograft recipients. Exp Clin Transplant 2015;13:145-151.
54 Ramirez GA, Coletto LA, Sciorati C, Bozzolo EP, Manunta P, Rovere-Querini P, Manfredi AA: Ion Channels and Transporters in Inflammation: Special Focus on TRP Channels and TRPC6. Cells 2018;7:pii:E70.

55 Park SK, Kang MJ, Kim W, Koh GY: Renal tubule regeneration after ischemic injury is coupled to the up-regulation and activation of cyclins and cyclin dependent kinases. Kidney Int 1997;52:706-714.
56 Qi S, Wu D: Bone marrow-derived mesenchymal stem cells protect against cisplatin-induced acute kidney injury in rats by inhibiting cell apoptosis. Int J Mol Med 2013;32:1262-1272.
57 Berger K, Moeller MJ: Mechanisms of epithelial repair and regeneration after acute kidney injury. Semin Nephrol 2014;34:394-403.
58 Hirschler-Laszkiewicz I, Tong Q, Conrad K, Zhang W, Flint WW, Barber AJ, Barber DL, Cheung JY, Miller BA: TRPC3 activation by erythropoietin is modulated by TRPC6. J Biol Chem 2009;284:4567-4581.
59 Liu BC, Song X, Lu XY, Li DT, Eaton DC, Shen BZ, Li XQ, Ma HP: High glucose induces podocyte apoptosis by stimulating TRPC6 via elevation of reactive oxygen species. Biochim Biophys Acta 2013;1833:1434-1442.
60 Zhang Y, Qin W, Zhang L, Wu X, Du N, Hu Y, Li X, Shen N, Xiao D, Zhang H, Li Z, Zhang Y, Yang H, Gao F, Du Z, Xu C, Yang B: MicroRNA-26a prevents endothelial cell apoptosis by directly targeting TRPC6 in the setting of atherosclerosis. Sci Rep 2015;5:9401.
61 Kubben FJ, Peeters-Haesevoets A, Engels LG, Baeten CG, Schutte B, Arends JW, Stockbrugger RW, Blijham GH: Proliferating cell nuclear antigen (PCNA): a new marker to study human colonic cell proliferation. Gut 1994;35:530-535.
62 Saifudeen Z, Marks J, Du H, El-Dahr SS: Spatial repression of PCNA by p53 during kidney development. Am J Physiol Renal Physiol 2002;283:F727-733.
63 Perucca P, Sommatis S, Mocchi R, Prosperi E, Stivala LA, Cazzalini O: A DDB2 mutant protein unable to interact with PCNA promotes cell cycle progression of human transformed embryonic kidney cells. Cell Cycle 2015;14:3920-3928.
64 Liu B, He X, Li S, Xu B, Birnbaumer L, Liao Y: Deletion of diacylglycerol-responsive TRPC genes attenuates diabetic nephropathy by inhibiting activation of the TGFbeta1 signaling pathway. Am J Transl Res 2017;9:5619-5630.
65 Saliba Y, Karam R, Smayra V, Aftimos G, Abramowitz J, Birnbaumer L, Fares N: Evidence of a Role for Fibroblast Transient Receptor Potential Canonical 3 Ca2+ Channel in Renal Fibrosis. J Am Soc Nephrol 2015;26:1855-1876.
66 Smedlund K, Vazquez G: Involvement of native TRPC3 proteins in ATP-dependent expression of VCAM-1 and monocyte adherence in coronary artery endothelial cells. Arterioscler Thromb Vasc Biol 2008;28:2049-2055.
67 Thilo F, Scholze A, Liu DY, Zidek W, Tepel M: Association of transient receptor potential canonical type 3 (TRPC3) channel transcripts with proinflammatory cytokines. Arch Biochem Biophys 2008;471:57-62.
68 Smedlund K, Tano JY, Vazquez G: The constitutive function of native TRPC3 channels modulates vascular cell adhesion molecule-1 expression in coronary endothelial cells through nuclear factor kappaB signaling. Circ Res 2010;106:1479-1488.
69 Smedlund KB, Birnbaumer L, Vazquez G: Increased size and cellularity of advanced atherosclerotic lesions in mice with endothelial overexpression of the human TRPC3 channel. Proc Natl Acad Sci U S A 2015;112:E2201-2206.
70 Riehle M, Buscher AK, Gohlke BO, Kassmann M, Kolatsi-Joannou M, Brasen JH, Nagel M, Becker JU, Winyard P, Hoyer PF, Preissner R, Krautwurst D, Gollasch M, Weber S, Harteneck C: TRPC6 G757D Loss-of-Function Mutation Associates with FSGS. J Am Soc Nephrol 2016;27:2771-2783.
71 Urban N, Wang L, Kwiek S, Rademann J, Kuebler WM, Schaefer M: Identification and Validation of Larixyl Acetate as a Potent TRPC6 Inhibitor. Mol Pharmacol 2016;89:197-213.
72 Urban N, Neuser S, Hentschel A, Kohling S, Rademann J, Schaefer M: Pharmacological inhibition of focal segmental glomerulosclerosis-related, gain of function mutants of TRPC6 channels by semi-synthetic derivatives of larixol. Br J Pharmacol 2017;174:4099-4122.
73 Hafner S, Burg F, Kannler M, Urban N, Mayer P, Dietrich A, Trauner D, Broichhagen J, Schaefer M: A (+)-Larixol Congener with High Affinity and Subtype Selectivity toward TRPC6. ChemMedChem 2018;13:1028-1035.
74 Koro CE, Lee BH, Bowlin SJ: Antidiabetic medication use and prevalence of chronic kidney disease among patients with type 2 diabetes mellitus in the United States. Clin Ther 2009;31:2608-2617.
75 Lizicarova D, Krahulec B, Hirnerova E, Gaspar L, Celecova Z: Risk factors in diabetic nephropathy progression at present. Bratisl Lek Listy 2014;115:517-521.

76 Zhou Y, Castonguay P, Sidhom EH, Clark AR, Dvela-Levitt M, Kim S, Sieber J, Wieder N, Jung JY, Andreeva S, Reichardt J, Dubois F, Hoffmann SC, Basgen JM, Montesinos MS, Weins A, Johnson AC, Lander ES, Garrett MR, Hopkins CR, et al.: A small-molecule inhibitor of TRPC5 ion channels suppresses progressive kidney disease in animal models. Science 2017;358:1332-1336.

77 Eckel J, Lavin PJ, Finch EA, Mukerji N, Burch J, Gbadegesin R, Wu G, Bowling B, Byrd A, Hall G, Sparks M, Zhang ZS, Homstad A, Barisoni L, Birbaumer L, Rosenberg P, Winn MP: TRPC6 enhances angiotensin II-induced albuminuria. J Am Soc Nephrol 2011;22:526-535.

78 Kim JH, Xie J, Hwang KH, Wu YL, Oliver N, Eom M, Park KS, Barrezueta N, Kong ID, Fracasso RP, Huang CL, Cha SK: Klotho May Ameliorate Proteinuria by Targeting TRPC6 Channels in Podocytes. J Am Soc Nephrol 2017;28:140-151.